Preprints of the 19th World Congress
The International Federation of Automatic Control
Cape Town, South Africa. August 24-29, 2014

On-Engine Validation of Mean Value Models for IC Engine Air-Path Control and Evaluation ⋆

Paul Dickinson * **Dariusz Cieslar** *,1 **Keith Glover** *
Nick Collings * **Yukio Yamashita** ** **Yusuke Yashiro** **
Toru Hoshi **

* *Dept. of Engineering, University of Cambridge, UK. (e-mail: pbd24@cam.ac.uk)*
** *Mitsubishi Heavy Industries, Ltd., Japan. (e-mail: yukio_yamashita@mhi.co.jp)*

Abstract: Mean value engine models (MVEM) are well established for the study of IC engine air-path performance. Closed-loop control of the air-path is used to ensure the tracking of reference signals subject to constraints. To meet these requirements model predictive control (MPC) has been applied successfully to several air-path applications. This paper reports on the development of an MVEM and suitable MPC controller for transient performance evaluation which is then applied to the engine. A linearised prediction model is evaluated at each control time step, based on the current operating conditions, which ensures the model remains valid across a wide range of speeds and loads. This linearisation of the nonlinear model allows for the formulation of quadratic programming (QP) problems, which are efficiently solved as part of the proposed MPC algorithm. Special treatment in the measurement and calculation of the states and their derivatives is demonstrated to provide excellent tracking performance and a good match between the model and real-time experimental results. The systematic process of modelling coupled with MPC is shown to closely match test-bed performance, which verifies the methodology for studying air-path hardware alternatives.

Keywords: Model-based control, Predictive control, Internal combustion engines, Transient response, Diesel engines.

1. INTRODUCTION

Engine downsizing is becoming increasingly common as one method of improving fuel economy and lowering tailpipe emissions. Pressure charging is used to recover the torque and power of an equivalent larger capacity normally aspirated engine. The smaller swept volume has benefits of improved thermodynamic efficiency and lower friction losses, both of which can improve with higher levels of downsizing. However, one of the challenges of using pressure charging on downsized engines is maintaining acceptable transient response, where at low engine speeds the air-path is unable to generate the equivalent mass flow of a larger normally aspirated engine. This torque 'deficit' and the inertia of the turbocharger leads to 'turbo-lag' in transients. To best mitigate this effect a significant amount of effort is put into the air-path design and selection of components. The vast majority of pressure charging systems use turbochargers and the selection process requires both steady state matching and transient considerations for the vast array of types and sizes available. For an overview of the range of boosting technologies available see Martinez-Botas et al. (2011).

Simulation models are valuable tools in the selection of the boosting system. Evaluation of the transient response is becoming increasingly important as levels of downsizing increase if acceptable driveability is to be maintained. With many boosting systems using actively controlled actuators there has been an increased interest in MPC for demonstrating the potential closed loop system performance for simulation purposes (Cieslar et al. (2014)). The benefits include the coordination of actuators and the ability to control within constraints without the need for a significant amount of tuning effort.

Validation of the simulations in an engine test cell is an important part of the hardware selection process. The air-path is subject to constraints including: maximum turbocharger speed, boost pressure, compressor outlet temperature and actuator limits, and therefore physical testing is useful to reassure the engineer of real-world performance. Moreover, whilst the simulation environment allows full state feedback, with the absence of noise this is not the case on the physical system and therefore, these limitations need to be addressed.

Although almost all engine control units (ECU) realise their production code in the form of scheduled PID controllers, the higher computational demands of MPC are not specifically addressed in this paper. Explicit MPC is

⋆ Work by P. Dickinson was funded by MHI. D. Cieslar was funded by the EPSRC Programme Grant EP/G066477/1
[1] Now at dSPACE Ltd., Melbourn, UK.

one approach to reduce the computation demand since there is no online optimisation and instead the performance is a trade-off in memory space of pre-computed solutions. In Zhao et al. (2013) the authors demonstrate an explicit MPC controller for the control of the VGT and EGR air-path actuators, as well as the fuel path, for modest transients. Stewart and Borrelli (2008) demonstrate an explicit MPC air-path controller on a 40 MHz MPC555 microcontroller with a 100 ms update rate.

Behrendt et al. (2011) investigated a real-time linear MPC torque tracking controller, which was successfully executed on a 150 MHz microcontroller with a control time step of 10 ms. The throttle and ignition demand were the manipulated variables and demonstrated to only use a fraction of the available time required showing the feasibility of real-time MPC on new generation ECUs.

Nonlinear MPC approaches to air-path control problems can be found in Ortner et al. (2009) and Herceg et al. (2006), which demonstrated modest improvements in performance relative to linear MPC approaches.

In the present paper a real-time linear MPC approach is applied that allows for efficient QP formulations which utilise full state feedback. If a certain sensor has a poor response time, a model is used as a state estimator. The purpose of this paper is to demonstrate a systematic procedure for hardware evaluation at the component selection stage, proving hardware performance and exploring the limitations due to air-path constraints. By studying a difficult transient, which covers a significant region of the engine operating map and is not necessarily close to its steady state equilibria, we aim to demonstrate a suitable match between the overall system behaviour of an MPC controlled simulation model and the test engine operating with the same controller.

2. EXPERIMENTAL SETUP

The engine used in this study was a 2.0 l light duty diesel engine designed to meet Euro V emissions regulation. The engine was fitted with a variable geometry turbine (VGT) turbocharger for the modelling part of the study and later replaced with a unit of different specification for testing and validation of the modelling and control methodology. The VGT vanes have pneumatic actuation, where the position is controlled by a feedback loop, which regulates the level of 'vacuum' applied to the actuator. The engine includes a high pressure exhaust gas recirculation (EGR) loop and the dynamics were used to validate the appropriate partitioning of the lumped volumes using the oxygen measurements (Cieslar et al. (2012b)). However, since this study focuses on turbo-lag, the tip-in validation manoeuvre under consideration assumes the EGR valve to be closed.

Pressure sensors and thermocouples were added in each of the identified lumped volumes of the engine, oxygen measurements in the intake and exhaust manifolds were made using modified UEGO sensors and a turbocharger speed sensor was fitted into the compressor housing. The engine layout is illustrated in Fig. 1 which shows the key instrumentation. Air and fuel mass flow values were collected from the ECU with the fuelling control being carried out using the standard ECU controller.

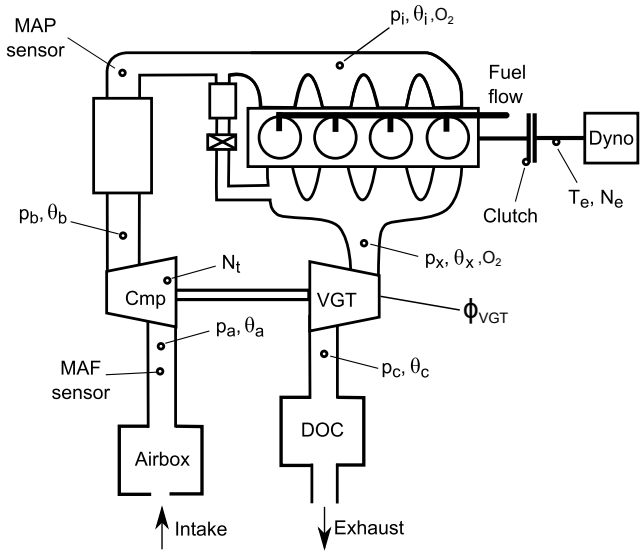

Fig. 1. Engine layout including key instrumentation.

A dSPACE rapid prototyping system was used for the data acquisition, dynamometer speed control and real-time MPC control. Control signals for actuation of the vane position of the VGT were passed to and from the ECU using a bypass process which uses the CAN calibration protocol (CCP). In this way the low level VGT vane position controllers could be utilised. The control model was run at a sample time of 1 ms for data acquisition, dynamometer control and signal filtering. The model linearisation and MPC was executed every 50 ms.

3. MEAN VALUE ENGINE MODEL

MVEMs have been widely accepted to capture the fundamental characteristics of air-path engine operation and are popular for their relative simplicity (both to develop and computationally). It is straightforward to capture an engine's dynamics and to subsequently study alternative air-path components such as different turbochargers.

The modelling described here is substantially the same as described in Guzzella and Onder (2009) and Cieslar et al. (2012a). The engine was lumped into five control volumes: pre-compressor, post-compressor, inlet manifold, exhaust manifold and post turbine.

Orifices: The orifice flow equation is used to model the mass flow w_{or} between control volumes.

$$w_{or} = \frac{A_{or} p_1}{\sqrt{R\vartheta_1}} \Psi\left(\frac{p_1}{p_2}\right) \tag{1}$$

where Ψ is defined as:

$$\Psi\left(\frac{p_1}{p_2}\right) = \tag{2}$$
$$\begin{cases} \left(\frac{p_2}{p_1}\right)^{\frac{1}{\gamma}} \left[\frac{2\gamma}{\gamma-1}\left(1-\left(\frac{p_2}{p_1}\right)^{\frac{\gamma-1}{\gamma}}\right)\right]^{\frac{1}{2}}, & \text{for } \left(\frac{p_2}{p_1}\right) > 0.528 \\ \gamma^{\frac{1}{2}}\left(\frac{2}{\gamma+1}\right)^{\frac{\gamma+1}{2(\gamma-1)}}, & \text{for } \left(\frac{p_2}{p_1}\right) \leq 0.528 \end{cases}$$

where p_1 and p_2 are pressures before and after the orifice, A_{or} is the effective area, ϑ_1 is the temperature of gas at the inlet, R is the universal gas constant and γ is the ratio of specific heats.

Control volumes: The control volumes are all modelled using the ideal gas law and the principles of conservation of mass and energy:

$$\frac{dp}{dt} = \frac{R\gamma}{V}\sum_j w_j\vartheta_j \tag{3}$$

$$\frac{dm}{dt} = \sum_j w_j \tag{4}$$

where V is the lumped volume of the particular air-path section, w_j are the gas mass-flows in and out with corresponding temperatures ϑ_j, and m is the mass of the gas stored in the volume at pressure p. The gases flowing out of the volume have a temperature determined by the ideal gas law:

$$\vartheta = \frac{pV}{mR} \tag{5}$$

Compressor and turbine: The compressor and turbine are modelled by three 2D maps, where the data necessary to populate the maps is extracted from the manufacturer's data. The maps f_{ϑ_r}, f_w and f_T give the temperature ratio, mass flow and torque parameters as functions of the speed parameter, $\tilde{N}_t$, pressure ratio and, in the case of variable geometry turbine, the VGT position ϕ:

$$\vartheta_r = f_{\vartheta_r}\left(\frac{p_2}{p_1}, \tilde{N}_t, \phi\right) \tag{6}$$

$$w = \frac{d_{ref}^2 p_1}{\sqrt{R\vartheta_1}} f_w\left(\frac{p_2}{p_1}, \tilde{N}_t, \phi\right) \tag{7}$$

$$T = \frac{d_{ref}^3 p_1}{R} f_T\left(\frac{p_2}{p_1}, \tilde{N}_t, \phi\right) \tag{8}$$

The speed parameter, $\tilde{N}_t$, is defined as follows:

$$\tilde{N}_t = \frac{d_{ref}}{\sqrt{R\vartheta_1}} N_t \tag{9}$$

where N_t is the turbine speed, ϑ_1 is the upstream gas temperature, p_1 and p_2 are pressures either side of the element with an effective flow reference diameter d_{ref}.

Turbocharger shaft dynamics: Turbocharger shaft dynamics are calculated from Newton's Second Law:

$$\frac{dN_t}{dt} = \frac{1}{J_t}\sum_j T_j \tag{10}$$

where J_t is the turbocharger inertia and T_j are the torques acting on turbocharger shaft from the compressor and turbine.

Coolers: There are two charge coolers in the modelled air-path: intercooler and EGR cooler. Both describe the outlet temperature ϑ_2 as a function of the coolant temperature ϑ_{cool} and the inlet temperature ϑ_1:

$$\vartheta_2 = \vartheta_1 - \eta_{cool}(\vartheta_1 - \vartheta_{cool}) \tag{11}$$

The cooler effectiveness is given by the parameter η_{cool}.

Engine block: The engine block is used to determine the brake torque, exhaust gas temperature, intake and exhaust mass flows. The flow from the intake manifold w_i is calculated from:

$$w_i = \eta_v(N_e, p_i)\frac{N_e n_{cyl} V_{cyl} p_i}{\pi R n_s \vartheta_i} \tag{12}$$

where the volumetric efficiency, η_v, is a map based on the engine speed, N_e, and inlet manifold pressure, p_i. The other parameters are: the number of cylinders, n_{cyl}, cylinder swept volume, V_{cyl}, the number of strokes per cycle, n_s and the inlet temperature ϑ_i. The exhaust mass flow is simply the sum of the fuel flow w_f and intake flow:

$$w_e = w_i + w_f \tag{13}$$

The brake torque T_B is calculated by subtracting the friction torque and transient pumping losses, ΔT_P, from the indicated torque. The friction torque, T_F, is modelled as a second order polynomial as a function of engine speed:

$$T_F = f_1 + f_2 N_e + f_3 N_e^2 \tag{14}$$

where the coefficients f_1, f_2 and f_3 are found from motoring tests. The indicated torque is found from steady state tests by subtracting the friction torque from the measured torque and modelled using:

$$T_I = \eta_z(\lambda)\eta_c(N_e, \bar{w}_f)\frac{w_f Q_{LHV}}{N_e} \tag{15}$$

where Q_{LHV} is the lower heating value for Diesel fuel. The combustion efficiency, $\eta_z(\lambda)$, is assumed to be 1 for a well calibrated engine at steady state but for $1 < \lambda < 1.2$, $\eta_z(\lambda)$ reduces from 1 to 0.85, as deduced from experiment. Fuel conversion efficiency, η_c, is a map scheduled on engine speed and fuel flow in milligrams per stroke.

In order to evaluate other air-path hardware there is an assumption that the friction coefficients and fuel conversion efficiency are strong functions of the engine (block and injection equipment) and are weak functions of the turbocharger hardware under consideration. The most significant changes to the engine torque from the air-path arise from the changes in exhaust and inlet manifold operating pressures. With different air-path hardware and during significant transient manoeuvres, the instantaneous pressures in the intake p_i and exhaust p_x manifolds can be very different from the steady-state values, $p_{i,ss}$ and $p_{x,ss}$ of the engine in its original hardware configuration. The difference in torque, ΔT_P, resulting from changes in pumping work relative to the original hardware at steady state can be reasonably approximated by:

$$\Delta T_P = \frac{(\Delta p_i - \Delta p_x) n_{cyl} V_{cyl}}{4\pi} \tag{16}$$

where

$$\Delta p_i = p_i - p_{i,ss}(N_e, \bar{w}_f) \tag{17}$$

$$\Delta p_x = p_x - p_{x,ss}(N_e, \bar{w}_f) \tag{18}$$

Exhaust gas temperature ϑ_e is calculated from the inlet temperature and the increase due to combustion using:

$$\vartheta_e = \vartheta_i + \eta_e(N_e, \bar{w}_f)\frac{w_f Q_{LHV}}{c_p w_e} \tag{19}$$

where the exhaust energy coefficient, η_e, accounts for the proportion of the fuel that heats the working fluid, mapped as a function of injection quantity and engine speed.

MVEM parametrisation: Parametrisation of the MVEM is largely from a set of steady state engine data over a

grid of engine speed and load points. The engine block coefficients are captured as 2D maps. The volume parameters required in the MVEM are obtained by dividing the air-path into the appropriate sections and summing up the individual component volumes. Turbocharger maps and inertia data were supplied by the manufacturer. The remaining parameters are the effectiveness of the coolers which were found to be sufficiently well described by constants.

3.1 Model verification

One of the benefits of the mean value modelling approach is the ability to simulate the engine with alternative components with minimal additional modelling effort. To validate this, the turbocharger on the engine was swapped to another specification and the turbocharger maps and inertia were changed accordingly. The engine was then exercised across a set of speed and load points.

The turbine actuator only operates within a subset of the manufacturers maps and therefore a function relating the measured VGT position to the appropriate space in the map was necessary. A linear relationship between the model and measured position was assumed and the coefficients were determined by using an optimisation which minimised the error of the sum of the squares of the differences in inlet and exhaust manifold pressures between the model and experiment respectively. The resulting function was found to be:

$$\phi_{model} = 0.05 + 0.77\phi_{measured} \tag{20}$$

After identifying the VGT calibration function the model was evaluated at each of the operating points using the measured inputs of VGT position, engine speed and fuelling (for this study the EGR was set to zero, i.e. closed). The model was found to match the measured results with satisfactory accuracy for all the variables used to determine the model state. An example of some of the model outputs is shown in Fig. 2. With only a few exceptions, the measured and modelled variables were found to be within 10% of each other with the exhaust pressure and post turbine temperatures displaying the largest difference. This fitness is comparable to other MVEMs reported in the literature (see for example Hadef et al. (2012)). It should be noted that the quality of fit with the originally modelled turbocharger was of similar quality, i.e. the fit was not observed to degrade when the turbocharger specification was changed. Despite the well-known difficulties in obtaining accurate turbocharger maps at low flow conditions, the level of fit demonstrated by the turbocharger speed plot appears to verify that model components can be exchanged without the need to model the entire system from scratch.

Transient torque estimation: The transient fit of the model was also found to be satisfactory for all but the torque prediction, where the simulated torque was higher than measured, particularly during large changes in torque. This result led to the introduction of the combustion efficiency term in (15) which is not commonly included in the literature. Whilst in steady state the engine operates at lean air-to-fuel ratios (e.g. $\lambda > 1.2$) where the combustion efficiency is almost 100%. However, during 'smoke limited' operation the measured AFR was much closer to stoichiometry. The torque measured during a

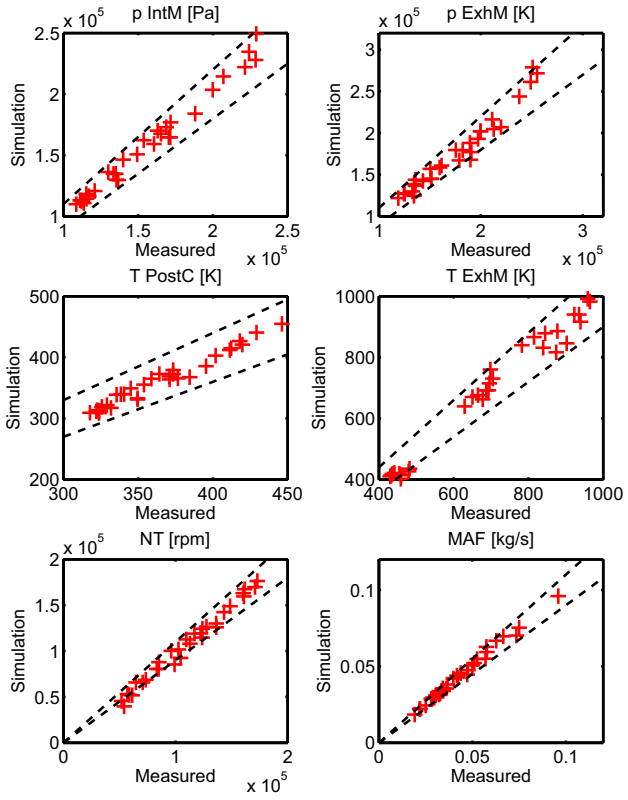

Fig. 2. Example of the steady state model fit. Dashed lines indicate 10% error bands.

tip-in manoeuvre, which exercises the engine from low to full load whilst the speed increases, is shown in Fig. 3. The smoke limited operation is clearly visible by the characteristic concave torque profile and the air-to-fuel ratio is seen to drop close to $\lambda = 1$. At this air-to-fuel ratio a significant amount of exhaust CO was measured, which provides evidence that the combustion efficiency was sub-optimal. Model A shows the torque model assuming a 100% combustion efficiency whereas Model B includes the combustion efficiency term as a function of λ.

3.2 Driveline model

Turbo-lag is most pronounced when accelerating the engine from low engine speeds (and therefore low mass flow conditions). A simple model of a vehicle and driveline was used to generate a representative load on the engine when simulating an in-gear vehicle acceleration. The driveline model used in this study considers only the longitudinal motion of the vehicle and wheel slip is assumed absent (Guzzella and Sciarretta (2005)). The only dynamic state is therefore the wheel speed N_{wh}:

$$\frac{dN_{wh}}{dt} = \frac{T_B r_{fdr} \eta_{fdr} r_g \eta_g - T_{brk} - F_{res} L_{rr}}{J_e r_{fdr}^2 r_g^2 + 4 J_{wh} + m_V L_{rr}^2} \tag{21}$$

where the inertia of the engine is J_e and the inertia of each wheel is J_{wh}. The total torque driving the wheels is calculated by subtracting the torque due to the braking system T_{brk} and the motion resistance torque $F_{res} L_{rr}$ from the propulsion torque. The latter is calculated by multiplying the engine torque T_B by the final drive ratio r_{fdr} and gear ratio r_g. Transmission losses are included via the differential efficiency η_{fdr} and gearbox efficiency η_g.

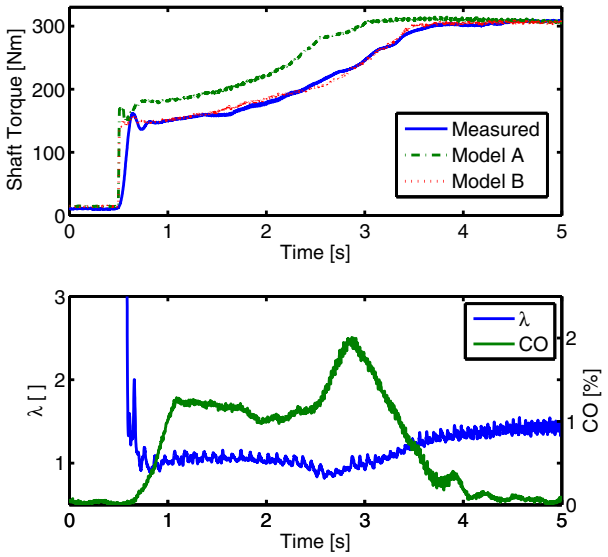

Fig. 3. Smoke limited operation showing generation of CO for $\lambda < 1.2$.

The motion resistance force is given by the sum of the rolling resistance F_{rr} and air drag F_a forces:

$$F_{rr} = C_{rr} m_V g \tag{22}$$

$$F_a = \frac{1}{2}\rho_a A_{fr} C_d (N_{wh} L_{rr})^2 \tag{23}$$

where C_{rr} is the rolling resistance coefficient, m_V the vehicle mass, g gravitational acceleration, ρ_a the density of air, A_{fr} the effective frontal area, C_d the air drag coefficient and L_{rr} the rolling radius of wheels.

Values for these parameters are taken from Fraser et al. (2009), which is based upon a European D-segment gasoline engine powered vehicle. In order to reduce the engine speed to match the Diesel engine's operating range, the final drive ratio was changed from 3.94 to 3. No other changes were considered necessary for a representative transient simulation.

The same driveline model was used to generate an appropriate speed command to the dynamometer dependent on the torque measured on the driveshaft, thereby reproducing in-vehicle behaviour.

4. REAL-TIME MPC

In this study, at each controller time step, the full nonlinear MVEM is linearised about the current state and input, to obtain the prediction model. The assumption here is that this linearised model will be valid as a prediction model for a limited number of time steps, albeit with increasing uncertainty further along the prediction horizon. The benefit of the linearisation is that it allows for the formulation of a QP problem for which efficient solvers exist. The result from each control step is applied at the current control instance and the process repeated at the next operating condition. This approach captures much of the model non-linearity without suffering the difficulties in optimising for a nonlinear model and has been successfully applied to similar problems (for example Darlington et al. (2012)).

The controller itself is executed every $t_s = 50$ ms and requires linearisation of the MVEM at the current operating point (x_0, u_0, d_0), discretisation of the linear model and solving the linear MPC optimisation problem. As the controller is being assessed during a transient manoeuvre, the model is not necessarily linearised around a steady-state operating point and therefore an offset $f(x_0, u_0, d_0)$ appears in the equations:

$$x_{k+1} - x_0 = f(x_0, u_0, d_0)t_s + A(x_k - x_0) + B_u(u_k - u_0) + B_d(d_k - d_0) \tag{24}$$

$$y_k - y_0 = C(x_k - x_0) \tag{25}$$

A matrix representing the system constraints was constructed to limit the maximum turbocharger speed, maximum boost pressure, maximum manifold pressure and actuator constraints. However, in this case it turned out that once the system weights relating to the rate of change of actuator and tracking penalty were tuned, only the actuator constraints remained active. Tuning of the penalty on the rate of change of actuator was a straightforward trade-off between an over-active actuator and damped response and was made relative to a fixed tracking penalty.

4.1 Model linearisation

The full nonlinear model is linearised at the current operating point using a finite differencing method and assumes the measured disturbances (fuelling and engine speed) remain constant for the given control execution period. The assumption that the load and speed are fixed means the prediction matrices are fixed, which simplifies the setup.

A more accurate model would be to linearise the MVEM along the trajectory predicted at the previous step. This would multiply the computational cost of the linearisation step by the length of the prediction horizon, however the QP would have the same dimensions.

5. IMPLEMENTATION AND RESULTS

The MPC was run on a high power DS1006 processor card with adequate processing power for the number of states, control horizon and prediction horizon therefore allowing the relative trade-offs in control performance to be studied. Nonetheless an efficient QP solver capable of running on the target device was required. An embedded M-coded solver was implemented in the Simulink model and autocoded to C using the Simulink coder. The solver used the dual active-set algorithm introduced in Goldfarb and Idnani (1983).

The prediction horizon and control horizons were set to 15 and 10 steps respectively. Increasing these was found to have a small negative effect on the result, since the prediction models became poor predictors for large numbers of steps in the future, and there was no computational requirement to make them shorter.

5.1 State feedback

In simulation it was assumed that all the measurements were instantaneous and noise free. On the engine the time

constant of the pressure sensor is such that the discrete engine pumping events are clearly evident and therefore some averaging of these signals is required. A 1st order low pass filter with a time constant equal to one engine cycle was chosen to achieve the best compromise between attenuation of high frequency and response time:

$$\tau = \frac{2\pi}{N_e} \tag{26}$$

The mass states in the model are a function of pressure and temperature. Temperature measurements were made with 1.6 mm thermocouples which have time constants of several seconds and therefore are not suitable to transient measurements. Accordingly, estimates of the instantaneous volumes temperatures were made. The volume pre-compressor was assumed to be at the ambient temperature. The temperature in the volume post-compressor was assumed to be equal to the compressor outlet temperature given in (7). Since the EGR valve was closed, there was no gas mixing to consider and therefore the inlet manifold temperature was estimated using the post-compressor temperature and the intercooler effectiveness (see (11)). The exhaust temperature was estimated based on the steady state block map given in (19) and the temperature in the volume post turbine obtained from the steady state turbine maps using (7).

5.2 State derivatives

The state derivatives used in the control algorithm were found to have a significant influence on the result. Over the 50 ms time step even relatively small errors in the predicted state could have a significant effect on the state derivatives due to the stiffness of the system. Therefore a pragmatic approach was to estimate the state derivatives directly from the state measurement at the current (t_0) and a previous time step ($t_0 - t_1$). At each time step the state derivative was estimated using:

$$\Delta x_0 = \frac{x(t_0) - x(t_0 - t_1)}{t_1} t_s \tag{27}$$

This significantly improved the controller performance and reduced the resulting steady state tracking error.

5.3 Tip-in manoeuvre

To best evaluate the effects of turbo-lag and the control system a 3rd gear tip-in manoeuvre was studied. This represents a driver suddenly demanding full engine torque from a relatively low engine speed, here 1150 rpm. When the pedal is depressed the fuelling is immediately increased up to the smoke limit (see Fig. 3). However, since the engine speed and inlet manifold pressure start from low levels there is insufficient air mass flow to immediately meet the driver's torque request. Accordingly, there is a smoke limited period whilst the turbocharger accelerates and the inlet manifold pressure increases. The control challenge is therefore to increase the inlet manifold pressure as quickly as possible, subject to any air-path constraints. For the engine in this study, the maximum boost pressure for steady state operation is 2.4 bar, which was set as the high load reference. When a full load tip-in event is detected it is standard for the EGR valve position demand to immediately close. For repeatability of the testing the EGR was set to closed before the start of the tip in.

5.4 Results

Figures 4 and 5 show the results of the MPC control of the engine in a test cell together with the simulation. A non-causal low pass filter has been applied to the measurements traces for clarity in viewing the results. At $t =$ 1 s the manoeuvre begins with the inlet manifold pressure initially at 1.06 bar. The controller immediately closes the vanes on the VGT to get the maximum acceleration of the turbocharger. As the pressure gets close to the demanded value, the VGT vanes begin to open, to prevent an overshoot in boost. As the vanes open the exhaust pressure stops increasing and the rate of turbocharger acceleration significantly reduces. Because the engine speed is continuing to accelerate the vanes continue to progressively open. The smoke limited period of the transient is clearly observed in the fuelling and corresponding torque traces.

Agreement between the test cell experiments and simulation results is good. It is noted that the system is relatively insensitive to vane position at low load and low mass flow conditions. The controller was tuned in simulation with no changes required to the MPC cost matrices as a result of the experiments. This result is particularly encouraging in indicating the modelled physical system dynamics closely match that of the engine. The control is less smooth than the simulation due to measurement noise. A larger weighting could have been applied to the rate of change of the actuator, however, this was deemed unnecessary due to the low pass filtering effect of the low level ECU position controller.

The simulated boost pressure rise slightly leads that measured on the engine. The lag on the engine test is believed to be due to a delay between the command to change the VGT and its actual position. Examination of the exhaust pressure shows that the simulated exhaust pressure rises much faster than the experiment, confirming that there is a delay in the VGT vane position moving to the requested set-point. This delay is in part due to the nature of CAN communication, which is non-deterministic between the rapid prototyping system and the ECU providing the low level control, and also, the ECU internal control structure. To further improve the control of the real-time system the VGT dynamics could be included in the prediction model.

Despite any modelling deficiencies, including the VGT dynamics, the match between the simulated transient and test-bed results strongly support the use of MVEMs with an appropriate controller for the study of the engine air-path dynamics. The original MVEM was developed using the standard approach which made a suitable platform to study other hardware.

6. CONCLUSIONS

An MVEM of a light duty diesel engine was constructed using steady state engine data for the study of air-path transients. The model was modified to capture the behaviour of an alternative VGT turbocharger by swapping the data for another specification of interest. The resulting model was demonstrated to have good steady state agreement with the engine.

The transient performance of the system was studied and optimised using MPC in simulation. The tuned controller

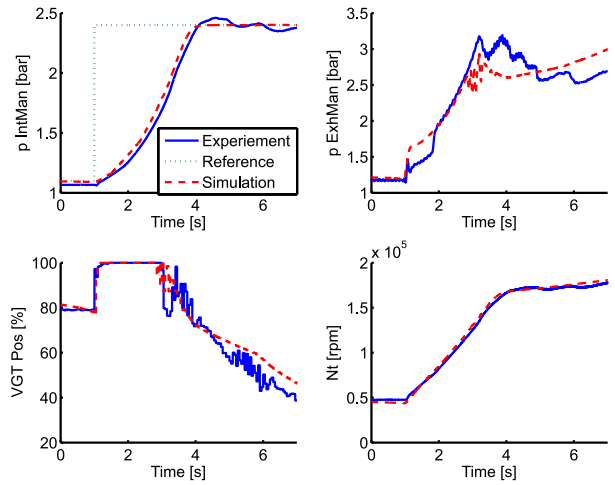

Fig. 4. Online and simulation signal traces during a 3rd gear tip-in (a).

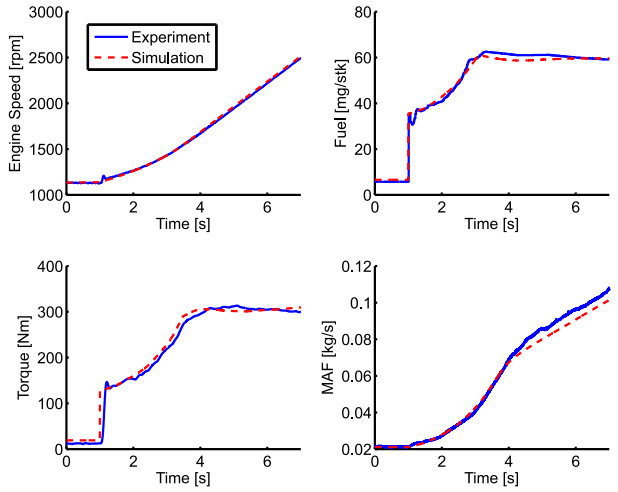

Fig. 5. Online and simulation signal traces during a 3rd gear tip-in (b).

was applied online and the engine shown to closely match the simulations without the need for any additional tuning. This validation demonstrates that an MVEM simulation environment is suitable for evaluating different air-path hardware options and that the control performance of MPC can be quickly and systematically realised on the test bench.

This systematic modelling and control approach is useful for evaluating hardware concepts through to proof of performance on the test bench.

ACKNOWLEDGEMENTS

The authors would like to acknowledge the contributions of Dr. Darlington for setting up this study and Dr. Hartley for providing the embedded Matlab QP solver.

REFERENCES

Behrendt, S., Dünow, P., and Lampe, B. (2011). An application of model predictive control to a gasoline engine. In *18th International Conference on Process Control*. Tatranska Lomnica, Slovakia.

Cieslar, D., Darlington, A., Glover, K., and Collings, N. (2012a). Model based control for closed loop testing of 1-D engine simulation models. *IFAC Engine and Powertrain Control, Simulation and Modeling*, 3(1).

Cieslar, D., Dickinson, P., Darlington, A., Hegarty, K., Collings, N., and Glover, K. (2012b). Mean-value oxygen concentration modelling and experimental validation using fast UEGO sensors. *Presented at Powertrain Modelling and Control Conf. Bradford*.

Cieslar, D., Dickinson, P., Darlington, A., Glover, K., and Collings, N. (2014). Model based approach to closed loop control of 1-d engine simulation models. *Control Engineering Practice*, (0). doi: http://dx.doi.org/10.1016/j.conengprac.2014.01.021.

Darlington, A., Cieslar, D., Glover, K., and Collings, N. (2012). Assessing boost-assist options for turbocharged engines using 1-D engine simulation and Model Predictive Control. *SAE Technical Paper*, (2012-01-1735).

Fraser, N., Blaxhill, H., Lumsden, G., and Bassett, M. (2009). Challenges for increased efficiency through gasoline engine downsizing. *SAE Technical Paper*, (2009-01-1053).

Goldfarb, D. and Idnani, A. (1983). A numerically stable dual method for solving strictly convex quadratic programs. *Mathematical Programming*, 27, 1–33.

Guzzella, L. and Onder, C. (2009). *Introduction to Modeling and Control of Internal Combustion Engines Systems - 2nd Ed.* Springer.

Guzzella, L. and Sciarretta, A. (2005). *Vehicle Propulsion Systems Introduction to Modeling and Optimisation*. Springer.

Hadef, J.E., Colin, G., Chamaillard, Y., and Talon, V. (2012). Turbocharged SI engine models for control. In *AVEC*. Republic of Korea.

Herceg, M., Raff, T., Findeisen, R., and Allgower, F. (2006). Nonlinear model predictive control of a turbocharged diesel engine. In *Computer Aided Control System Design, IEEE International Symposium on Intelligent Control*. Munich, Germany.

Martinez-Botas, R., Pesiridis, A., and MingYang, Y. (2011). Overview of boosting options for future downsized engines. *Science China Technological Sciences*, 54(2).

Ortner, P., Bergmann, R., Ferreau, H.J., and del Re, L. (2009). Nonlinear model predictive control of a diesel engine airpath. In *IFAC Workshop on Control Applications of Optimization*, volume 7.

Stewart, G. and Borrelli, F. (2008). A model predictive control framework for industrial turbodiesel engine control. In *47th IEEE Conference on Decision and Control*.

Zhao, D., Liu, C., Stobart, R., Deng, J., Winward, E., and Dong, G. (2013). An explicit model predictive control framework for turbocharged diesel engine. *IEEE Transactions on Industrial Electronics*, 99.